Universal Journal of Catalysis Science
https://ojs.wiserpub.com/index.php/UJCS/

Research Article

Catalytic Performance of Pd/Al_2O_3 Catalyst in the Presence of HHDMA Ligand in Acetylene Selective Hydrogenation Process

Maryam Takht Ravanchi*, Maryam Rahimi Fard, Hadi Moosavi, Saeed Sahebdelfar

National Petrochemical Company, Petrochemical Research and Technology Company, Tehran, Iran
E-mail: maryamravanchi@gmail.com , m.ravanchi@npc-rt.ir

Received: 22 September 2023; **Revised:** 6 November 2023; **Accepted:** 10 November 2023

Abstract: A series of Pd-HHDMA/Al_2O_3 catalysts were prepared with various Pd and hexadecyl-2-hydroxyethyl-dimethylammonium dihydrogen phosphate (HHDMA) amounts by the reduction-deposition method. The catalysts were characterized by N_2-physisorption, FE-SEM, CO-TPD, TG and FT-IR techniques. Performance tests for tail-end semi-hydrogenation of acetylene to ethylene were performed in a fixed-bed reactor at 60 °C, 10 bar and GHSV=4000 h^{-1}. All catalysts exhibited egg-shell Pd distribution which is beneficial for selective semi-hydrogenation reaction. The BET surface area and pore volume of the catalysts decreased with increasing HHDMA content for a given Pd loading. The conversion of acetylene increased with Pd loading and decreased with HHDMA content. The ethylene production increased with HHDMA whereas that of undesirable C_{4+} oligomerization products ("green oil"), which are coke precursors, was effectively suppressed.

Keywords: acetylene selective hydrogenation, Pd nanocatalyst, reduction-deposition synthesis, HHDMA ligand, catalysis

1. Introduction

During the past decades, researchers have been focusing on the subject of semi-hydrogenation, because of its relevance in polymer industries and fine chemicals production [1]. The chemo- and stereo-selectivity of the catalyst plays a vital role in suppressing undesirable over-hydrogenation and oligomerization reactions. In olefin plants, acetylene is the poison for downstream polymerization catalyst; hence, its trace amounts in ethylene stream must be removed by selective hydrogenation process. Vilé et al. [2] reported a comprehensive list of selective hydrogenation reactions accompanying their respective catalysts.

In catalytic acetylene hydrogenation, dissociative chemisorption of H_2 is occurred at first and then hydrogen atoms are sequentially added to acetylenic substrate and consequently ethylene and ethane are produced by semi-hydrogenation and over-hydrogenation, respectively [3]. The formation of unwanted oligomers is also possible. Hence, the preferred selective catalyst is the one that adsorbs and hydrogenates the reactants and restricts the successive hydrogenation of products [4].

Recently, single-atom and sub-nanometer Pd clusters received much attention as highly active and selective catalysts for alkyne semi-hydrogenation. Pd^0 atoms (possibly coordinated with solvent and/or reactants) resulted from a palladium salt and hydrogen in alcohols, for example, showed exceptionally high turn-over frequencies and yields (up to ~99%) in alkyne semi-hydrogenation [5]. Similarly, Pd-$(CaCO_3)_n$ (n=2-13) clusters with single or few Pd atoms in solution or on solid supports showed one order of magnitude higher activity compared to the counterpart commercial catalysts [6].

Copyright ©2023 Maryam Takht Ravanchi, et al.
DOI: https://doi.org/10.37256/ujcs.1220233691
This is an open-access article distributed under a CC BY license
(Creative Commons Attribution 4.0 International License)
https://creativecommons.org/licenses/by/4.0/

Although palladium is the preferred active metal for acetylene hydrogenation [7], the challenging step is ending the reaction at favourable product steps; due to its high activity in hydrogen splitting. Intrinsically, palladium has low kinetic and thermodynamic selectivities and at moderate to high partial pressures of hydrogen, hydrides are formed by incorporation of H species into the Pd lattice [8]. Consequently, unfavourable hydrogenation side-reactions occur and oligomers are produced. Different strategies have been adopted to overcome this drawback including the use of alloys and intermetallic compounds (e.g., Pd-Ga), ligand modified nanoparticles, supported single atom catalysts, alternative metals and transition metal oxides (e.g., In_2O_3) [9]. In the presence of coke and carbon, Pd carbide phases are formed due to which activity is decreased and selectivity is increased [10].

The application of ligands has been proposed in catalyst synthesis stages to tailor atom size, suppress hybrid and carbide formation and to secure a high product yield [11].

In contrast to traditional impregnation method, the so-called reduction-deposition method based on suspension of colloids produces uniform (<10 nm) metal crystallites which are comparable in size with those obtained by traditional method but they lack large metallic particles [12]. In the presence of stabilizer, catalysts are synthesized by the reduction of metal precursor and its subsequent deposition on the support. The presence of ligands in catalyst synthesis has electronic and geometric effects as they tune the energy landscape of reactants and products and also, they isolate active sites.

Hexadecyl-2-hydroxyethyl-dimethylammonium dihydrogen phosphate ($C_{20}H_{46}NO_5P$, HHDMA) is an example of these ligands. It is a commercial chemical developed by BASF company as a ligand that is soluble in water and can be used in the synthesis of metal nanoparticles. The simultaneous compilation of stabilization and reduction characteristics in one molecule and its water solubility, make HHDMA ligand being applicable in commercial catalyst productions. In the presence of this ligand, Pd ensemble size was limited and potential oligomerization pathways were blocked [13].

Albani et al. [14] reported their research results for Pd-nanoparticle synthesis in the presence of HHDMA ligand and its subsequent impregnation on titanium silicate support and evaluated its performance for selective hydrogenation of C_6 hydrocarbons. In their research, HHDMA concentration was studied in the range of 0.3-16.8 wt.%. They reported that at 90 ^oC and 1 bar, 1-hexyne conversion rate was in the range of $1.1\text{-}2.9 \times 10^3$ h^{-1}.

For stabilizing Pd nanoparticles on TiS support, in the presence of HHDMA ligand, Witte et al. [15] proposed a mechanism according to which, Pd nanoparticles interacts with the support by polar head groups of HHDMA. A same mechanism is applicable for the interaction between free HHDMA and support.

The aim of this research is evaluating the presence of HHDMA in Pd/Al_2O_3 catalyst and its subsequent performance in tail-end acetylene selective hydrogenation process. The spent catalysts were characterized for coke amount and coke type as well. To the best of our knowledge, there is no published manuscript in which HHDMA ligand was used in the synthesis of alumina supported catalyst. Moreover, there is not any published research about the evaluation of these catalysts for acetylene selective hydrogenation process.

2. Materials and methods

2.1 *Chemicals*

A spherical γ-alumina (with 1.8-2 mm diameter, 0.5 cm^3/g pore volume and 210 m^2/g surface area) supplied from Sasol Co., was heat treated at 1090 ^oC and used as catalyst support.

Sodium chloropalladate (Na_2PdCl_4) supplied from Merck Co. was used as palladium precursor. HHDMA ligand was supplied from Sigma Co. All chemicals were of analytical grades and used without any extra purification step.

Gas mixture cylinder of acetylene-ethylene (containing 1.5 mol.% acetylene and 98.5 mol.% ethylene) and pure cylinders of hydrogen and nitrogen (containing > 99.9 mol.% gas) were supplied from Pars Havaye Alborz and used as reactant gases.

2.2 *Catalyst Synthesis*

Palladium nanocatalysts containing 0.15 and 0.3 wt.% of HHDMA ligand (as the stabilizer) were synthesized by the reduction-deposition method. At first, a pre-determined amount of Na_2PdCl_4 and HHDMA were dissolved in deionized water. NaOH solution (0.2 M) was added to the obtained solution in a dropwise manner until pH was adjusted to 4.0. Then the solution was heated to 85 ^oC for 2 hours. In the subsequent step, the obtained solution

was impregnated on alumina support for 2 hours at 25 ºC in a rotary. Then, the obtained sample was washed with deionized water, dried overnight and calcined at 250 ºC for 3 hours.

Mono-metallic Pd-HHDMA/Al_2O_3 catalysts were synthesized by the following procedures:

- *Sample A*: impregnating the solution containing 0.03 wt.% Pd and 0.15 wt.% HHDMA on alumina support.
- *Sample B*: the same as sample A but with 0.3 wt.% HHDMA.
- *Sample C*: the same as sample A but with palladium solution containing 0.06 wt.% Pd.
- *Sample D*: the same as sample C but with 0.3 wt.% HHDMA.
- *Sample E*: the same as sample A but with palladium solution containing 0.09 wt.% Pd.
- *Sample F*: the same as sample E but with 0.3 wt.% HHDMA.
- *Sample G*: the same as sample A but without HHDMA.

2.3 *Catalyst Characterization*

An X-ray diffractometer (GNRMPD 3000) with CuKa radiation of 30 mA and 40 kV was used to evaluate XRD patterns of alumina supports in 2θ range of 5-80º.

At 77 K, N_2 physisorption analysis by Quanta Chrome Nova 2200 analyser was used to characterize surface area of the synthesized samples. The pore size distribution was determined by the Barrett-Joyner-Halenda (BJH) method.

To evaluate palladium penetration depth, FESEM characterization test was conducted on synthesized samples by MIRA3TESCAN apparatus. At first, one pellet was polished on the top surface until half of the active Pd shell was observed; then it was coated with a layer of gold and transferred to microscope for analysis. A 15 kV electron beam under high vacuum condition was used during analysis.

BELCAT A apparatus was used for CO-TPD analysis, in which 0.2 g of catalyst sample was reduced for 2 hours at 150 °C by hydrogen, then the reactor was purged with helium at 150 °C for 1 hour (to remove the adsorbed hydrogen molecules from palladium surface). In the next step, the sample was exposed to CO at 40 °C and temperature was raised in the range of 40-700 °C with 10 °C/min heating rate.

For thermogravimetric characterization test, Perkin Elmer SII (Diamond TG/DTA) apparatus was used, by which fresh and spent samples were analysed in temperature range of 25-600 ºC with scanning rate of 5 ºC/min and in the presence of air.

Using Bruker spectrometer (Vortex 80) for fresh and spent catalysts, chemical structure of deposited coke was determined by FT-IR analysis. At first, self-supporting discs of each sample was prepared with KBr. Then, in the wavelength range of 4000-400cm^{-1}, FT-IR spectrum was recorded.

2.4 *Reaction Study*

All synthesized samples were evaluated in acetylene selective hydrogenation (tail-end) process by a high-pressure set-up described elsewhere [16].

For each catalytic test, gas mixture containing 1 mol.% acetylene, 1.5 mol.% hydrogen, 44 mol.% ethylene and 53.5 mol.% nitrogen was used as feed stream. At the beginning of the performance test, catalyst was reduced in-situ with hydrogen stream at 150 ºC for 4 hours at GHSV of 500 h^{-1}. Then, the reactor was cooled down to 60ºC by nitrogen stream. Catalytic performance of each sample was conducted at 60 ºC temperature, 10 bar pressure and GHSV of 4000 h^{-1}. Feed and product streams were analysed by an online GC apparatus (Varian-CP-3800), containing FID and TCD detectors. In the present research, the absence of mass and heat transfer limitations were checked at the applied operating conditions [17].

Catalytic performance of each synthesized sample was evaluated in terms of acetylene conversion (Eq. 1), ethylene production (consumption) (Eq. 2) and C_{4+} production (Eq. 3):

$$acetylene\ conversion = \frac{(C_2H_2)_{in}-(C_2H_2)_{out}}{(C_2H_2)_{in}} \times 100 \quad (1)$$

$$ethylene\ production\ (consumption) = \frac{(C_2H_4)_{out}-(C_2H_4)_{in}}{(C_2H_4)_{in}} \times 100 \quad (2)$$

$$C_{4+}\ production = \frac{(C_{4+})_{out}-(C_{4+})_{in}}{(C_{4+})_{in}} \times 100 \quad (3)$$

3. Results

3.1 *Support pre-treatment*

At first, spherical γ-alumina was calcined at 1090 °C with heating rate of 5 °C/min for 3 hours in an electrical furnace. The resulting support had 44 m^2/g BET surface area and 0.4 cm^3/g pore volume. According to XRD analysis this support comprised of θ-Al_2O_3 (20%) and α-Al_2O_3 (80%) phases, the spectra of which is depicted in Figure 1.

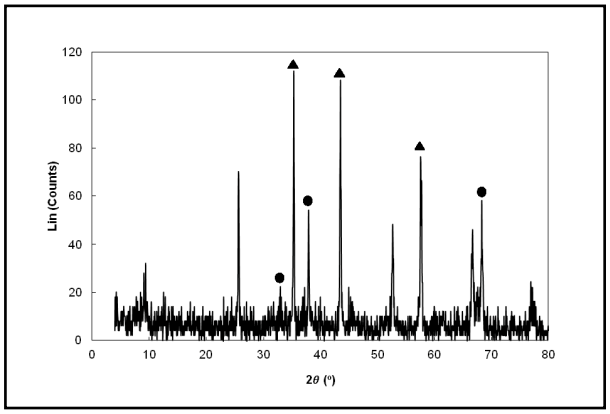


Figure 1. XRD graph of the heat-treated support; filled circles shows characteristic peaks for θ-Al_2O_3 and filled triangle denotes characteristic peaks for α-Al_2O_3

3.2 *Catalyst Characterization*

Catalyst surface area and Pd penetration depth, reported in Table 1, were evaluated by BET and FE-SEM analysis, respectively.

As it is observed in Table 1, due to the addition of Pd precursor and HHDMA ligand to the support, BET surface area of the resulting catalysts ranged from 50.40 m^2/g to 27.22 m^2/g (depending on Pd and HHDMA concentration). In low Pd- and HHDMA-containing samples (i.e., samples A, B and G), the surface area is slightly larger than that of the support which might be due to partial dissolution of the support during preparation. Furthermore, increasing HHDMA concentration decreased the BET surface area and this decrease in surface area was more obvious for samples with higher Pd contents. This finding is due to the presence of ligand molecule on support surface and Pd nanoparticles. Similarly, for a constant ligand content, increasing Pd concentration caused a decrease in catalyst surface area. As such, the lowest surface area was observed for the sample in which both metal and ligand amounts were highest (i.e., sample F).

Table 1. Catalyst surface area and Pd penetration depth of catalyst samples

Sample	Surface area (m^2/g)	Pd penetration depth (μm)
A	46.85	15.41
B	46.18	21.08
C	37.81	16.23
D	32.06	20.00
E	36.61	22.17
F	27.22	19.47
G	50.40	20.01

According to FE-SEM images (depicted in Figure A1), all samples exhibited egg-shell Pd distribution that is a pre-requisite for selective semi-hydrogenation reactions. When 0.15 wt.% of HHDMA was used (i.e., samples A, C and E), increasing Pd concentration caused a slight increase in Pd penetration depth, but when 0.3 wt.% of HHDMA was used (i.e., samples B, D and F) increasing Pd content did not have significant impact on Pd penetration depth (Table 1).

From BET characterization analysis, adsorption-desorption isotherms for the synthesized samples are reported in Figure 2. As it is obvious in Figure 2a, due to the presence of HHDMA ligand, macroporous structure of alumina support is not changed and according to BDDT classifications [18], all samples have isotherm type III with hysteresis loop type H4 and HHDMA concentration has no impact on hysteresis loop type.

According to BJH mesopore size distribution (Figure 2b), in the presence of HHDMA ligand, two-peak distributions were observed that means the presence of two types of pores. When Pd concentration was increased to 0.06 and 0.09 wt.%, the two-peak structure became more evident. On the other hand, for the samples containing 0.03 wt.% Pd, HHDMA concentration has no impact on pore diameter; but for samples containing 0.06 and 0.09 wt.% Pd, increasing HHDMA concentration decreased pore diameter.

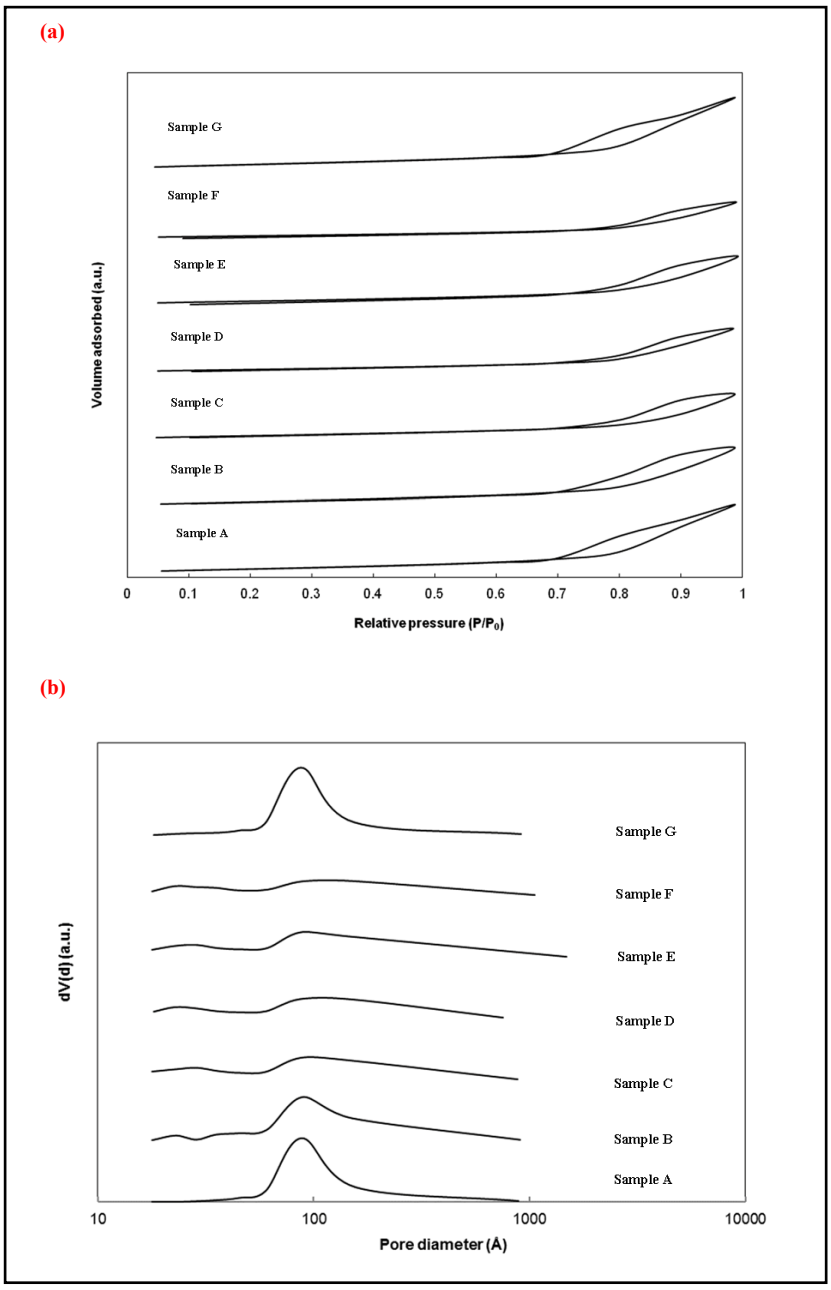


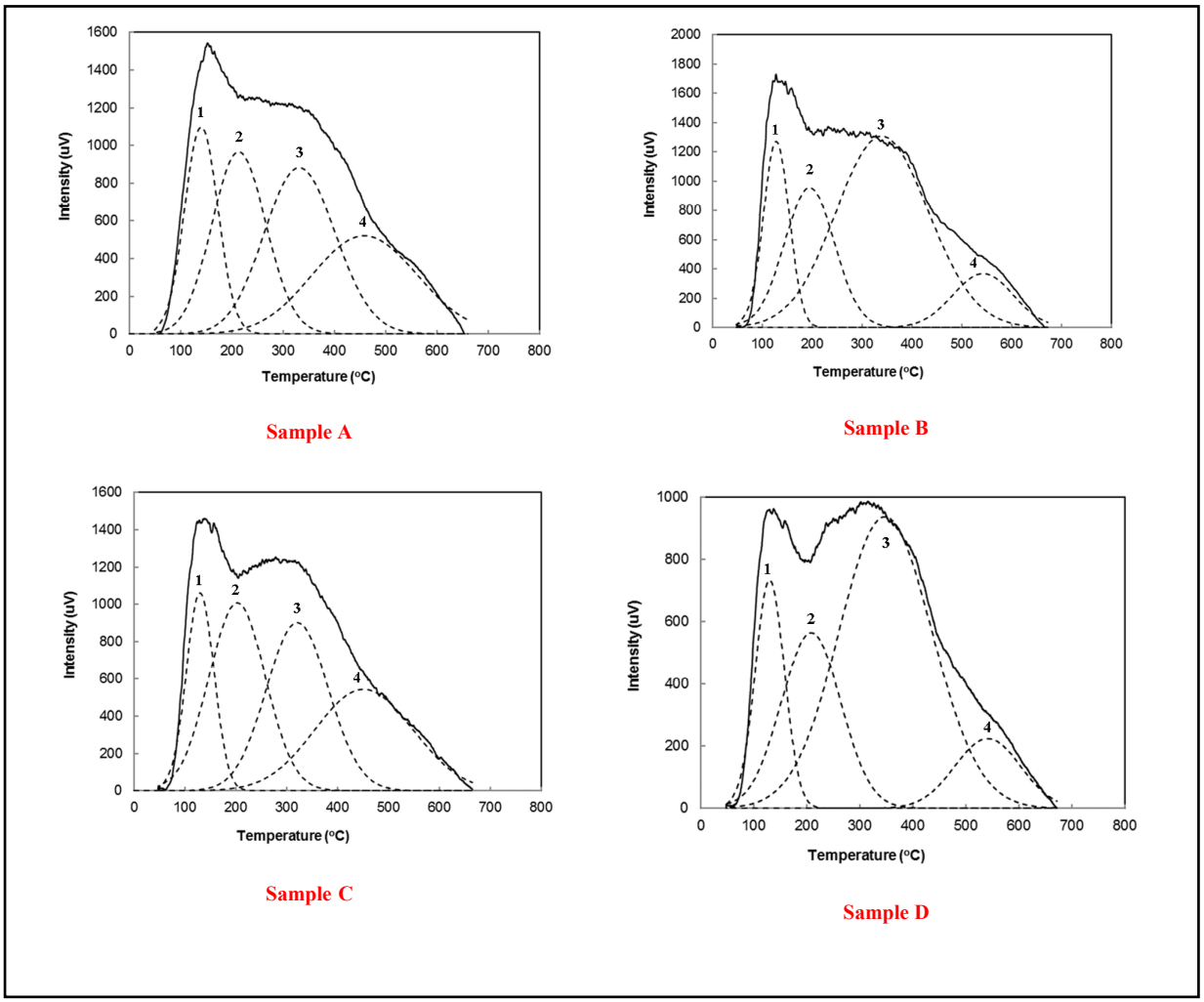
Figure 2. N_2 adsorption-desorption isotherms (a) and BJH graphs (b) of the synthesized samples

Therefore, one can conclude that for a given Pd loading, the apparent pore volume and pore diameter of the catalysts decrease with HHDMA which can be attributed to the coverage of pore walls with the relatively large ligand molecules.

In order to evaluate palladium active sites of the synthesized samples, TPD-CO analysis was used. Each spectrum and its specification are tabulated in Figure 3 and Table 2, respectively. As it is obvious, all HHDMA containing samples have four desorption peaks. The first peak is related to those CO species that are linearly bounded to surface Pd sites and the other peaks are assigned to those CO species that are multiply bounded to large palladium ensembles [19, 20]. Linear adsorption, as the favourable mode, occurred on Pd atoms that are isolated and multiply-bound adsorption happened on Pd ensembles that are adjacent together.

Table 2. TPD-CO results for catalyst samples.

Peak	Maximum peak temperature (°C)	CO adsorption (μmol/g)	Maximum peak temperature (°C)	CO adsorption (μmol/g)
	Sample A		*Sample B*	
1	139	48	126	40
2	213	67	194	58
3	331	77	338	144
4	458	64	542	26
total	-	256	-	268
	Sample C		*Sample D*	
1	129	36	129	25
2	202	70	208	39
3	321	68	347	101
4	461	63	541	16
total	-	237	-	181
	Sample E		*Sample F*	
1	126	7	129	55
2	174	18	201	43
3	268	38	340	77
4	391	27	535	45
total	-	90	-	220
	Sample G			
1	119	47		
2	170	103		
3	270	187		
4	398	118		
5	529	34		
total	-	489		



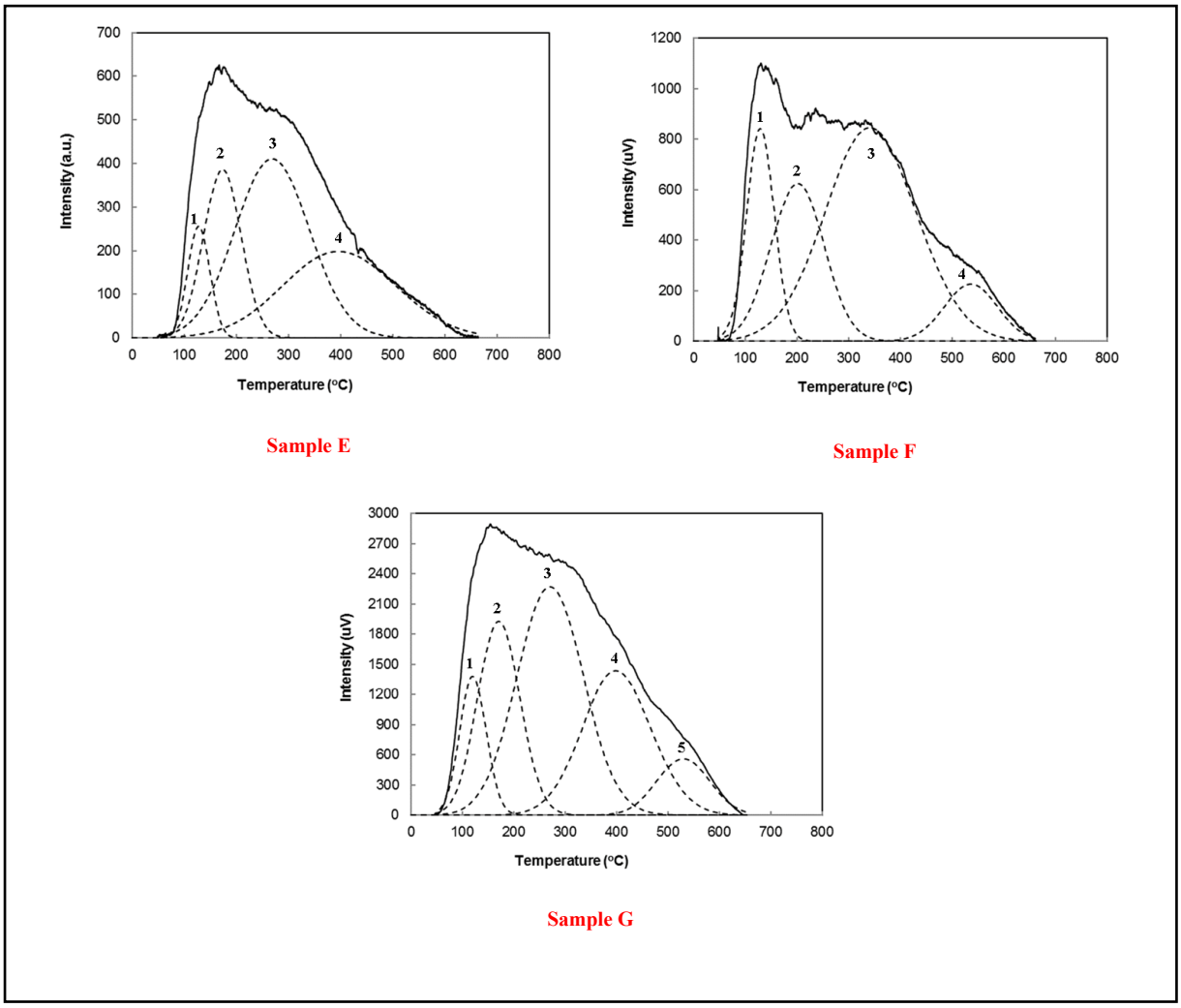


Figure 3. TPD-CO graphs of the synthesized samples

According to Table 2, when 0.15 wt.% of HHDMA ligand was used (i.e., samples A, C and E), by increasing Pd content from 0.03 to 0.09 wt.%, first peak was moved to lower temperature that is equivalent to weakening CO adsorption. When 0.3 wt.% of HHDMA ligand was used (i.e., samples B, D and F) the trend was vice versa that showed strengthening CO adsorption.

The most significant influence of ligand is reducing Pd ensembles. As it is observed in TPD-CO results, all ligand-containing samples have four desorption peaks while sample G (that is ligand-free) has five desorption peaks. Moreover, CO consumption of sample G was the highest.

3.3 *Catalyst Performance*

Catalytic performance of the synthesized samples was presented in Table 3, in terms of acetylene conversion, ethylene production (consumption) and C_{4+} production. As it is observed, at constant HHDMA concentration, increasing Pd content caused an increase in acetylene conversion and ethylene production. On the other hand, increasing ligand content, caused a decrease in acetylene conversion.

In Table 3, the data reported in parenthesis showed net ethylene consumption. As it is observed, in the absence of HHDMA ligand (sample G), the highest amount of ethylene consumption (via deep hydrogenation) was obtained but when HHDMA was added to catalyst, ethylene consumption was reduced and net ethylene production (via semi-hydrogenation) was observed.

A comparison between the results reported in Table 3 for ethylene production (consumption) revealed that increasing Pd content and HHDMA content has a positive effect on ethylene production that is a sign for improvement in ethylene selectivity.

Table 3. Catalytic performance of the synthesized samples (GHSV=4000 h^{-1}, P=10 bar, T=60 ºC, H_2:C_2H_2=1.5)

Sample	Acetylene conversion (%)	Ethylene production (consumption) (%)	C_{4+} (mol.%)
A	39.30	(0.99)	0.04
B	33.27	(0.72)	0.02
C	53.87	(0.02)	0.03
D	36.61	1.61	0
E	83.65	1.82	0
F	39.02	1.86	0
G	99.41	(3.01)	0.09

From the viewpoint of HHDMA amount, at constant Pd content, increasing the amount of HHDMA ligand caused a decrease in acetylene conversion. This is a logical result as the higher the ligand content, the lower the available Pd active sites and consequently acetylene conversion was decreased. Furthermore, the bulky organic tail of the ligand molecules can impose some limitation to the accessibility of Pd active sites by acetylene molecules.

C_{4+} are precursors for the formation of coke and green oil (by subsequent oligomerization reactions). As it is observed in Table 3, sample G has highest amount of C_{4+} production and in the presence of HHDMA ligand, C_{4+} production was decreased. This finding confirmed the positive effect of HHDMA ligand that consequently increases catalyst life time.

Factors increasing the adsorption of semi-hydrogenation product bring about further hydrogenation to complete saturation. DFT studies [21] revealed that the adsorbed amine ligand decreases alkene adsorption and affect adsorption configuration and thus blocks complete saturation sites thereby improves alkene selectivity in the hydrogenation products. They also exhibit beneficial effects by the geometric effect of site isolation [1].

3.4 *Coke Formation*

For Pd/Al_2O_3 catalysts, coke formation is the general deactivation mechanism. Fresh and spent samples (after being 24 hours on reaction) were characterized by TG analysis to evaluate ligand thermal stability and coke formation (Table 4). The DTG profiles of the fresh catalysts showed two peaks (Figure 4a). A sharp peak was observed at about 60 °C and a broad inconspicuous one at about 300 °C. As the support was calcined above 1000 °C, none of these peaks could be assigned to the dehydration (i.e., structural water loss) of the alumina support. The first peak is due to the loss of physisorbed water from pore structure. The second one is related to ligand decomposition showing a low intensity due to the small amount of the ligand employed. Previous studies reported that the dissociation of HHDMA ligand begins from 230 to 260 °C over a $TiSi_2O_6$ support [14].

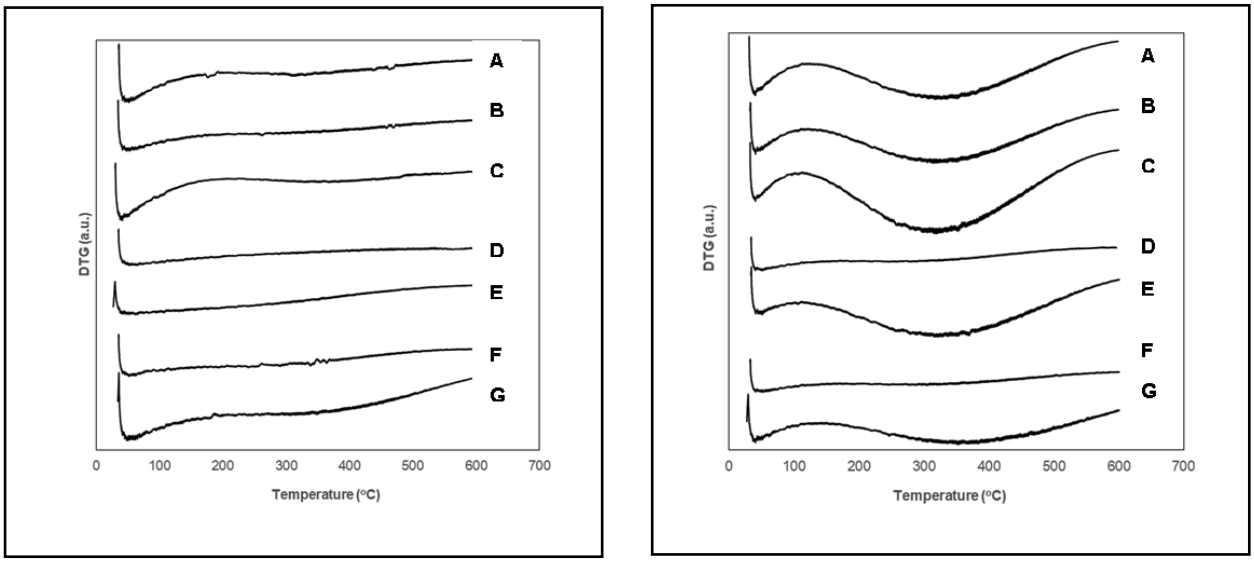


Figure 4. DTG of fresh (a) and spent (b) samples

Similarly, the DTG profiles of the spent catalysts show two peaks at nearly the same positions of fresh samples with the high temperature one (320 to 350 °C), being attributed to coke removal is much more prominent (Figure 4b). Consequently, the weight loss of the spent catalyst in 200-400 °C is directly proportional to the ligand content and the amount of coke deposited on catalyst [22-24]. A comparison with corresponding fresh catalysts profiles reveals that the former has a minor role.

Table 4 and Figure 4 illustrated that the lowest coke amount formed on sample F in which both metal loading and ligand loading were highest, meaning a large number of isolated Pd sites. The catalyst consistently showed the highest ethylene productivity as well (Table 3).

As catalyst performance was evaluated at 60 ºC and TG graphs did not show any significant weight loss at this temperature, it is concluded that ligand is in the structure of the catalyst and it did not leave the catalyst at reaction conditions.

TG profiles (not reported here) have similar trend for all synthesized samples that prove the presence of similar coke on all samples with various intensity. On the other hand, any increase in HHDMA content, cause a decrease in the amount of formed coke (Table 4).

Table 4. Weight loss during TG analysis for fresh and spent samples

Sample	Weight loss (%)			
	Fresh catalyst		Used catalyst	
	100-200 ºC	200-400 ºC	100-200 ºC	200-400 ºC
A	0.8	1.2	1.0	2.6
B	0.7	1.3	0.9	2.6
C	0.4	0.9	1.1	3.5
D	0.6	1.1	0.6	0.9
E	0.8	1.0	1.1	2.9
F	0.7	1.1	0.7	1.2
G	1.2	1.6	1.0	2.5

FT-IR analysis (Figure 5) was used to determine coke type. As it is obvious in Figure 5, the spectra of fresh and spent catalysts have specific differences; vibrations in the range of:

- 700-400 cm^{-1}: pseudo-boehmite structural vibrations and constitutive structure of α-alumina support
- 800-400 cm^{-1}: Al-O bond in alumina structure [25, 26].
- 800-600 cm^{-1}: C-H aromatic bond.
- 1800-1600 cm^{-1}: aromatic coke.
- 2000-1500 cm^{-1}: H-O-H bond vibration
- 3000-2800 cm^{-1}: the presence of HHDMA molecule on the surface of fresh catalysts; aliphatic coke of spent catalysts.
- 3800-3000 cm^{-1}: hydroxyl (OH^-) group [26, 27].
- 3600-3400 cm^{-1}: OH stretching bond.

The FT-IR results reveal the predominance of aliphatic coke on spent catalysts which is consistent with the DTG results.

The aliphatic coke can be easily removed by regeneration treatment of the spent catalyst. However, industrial regeneration is performed by controlled burning of the deposited coke with oxygen in the temperature range of 400-500 ºC which can also remove the ligand as illustrated by DTG results. Thus, the spent catalyst cannot be regenerated with the traditional procedure of industrial plants. Due to low thermostability of HHDMA ligand, development of alternative non-destructive methods such as coke leaching and coke extraction is required for the regeneration of the catalysts under mild conditions [28].

Although the catalysts showed good stability in liquid-phase operation (that is, little or no leaching of Pd and ligand) [14], more investigation is required as the leaching process is solvent–dependent.

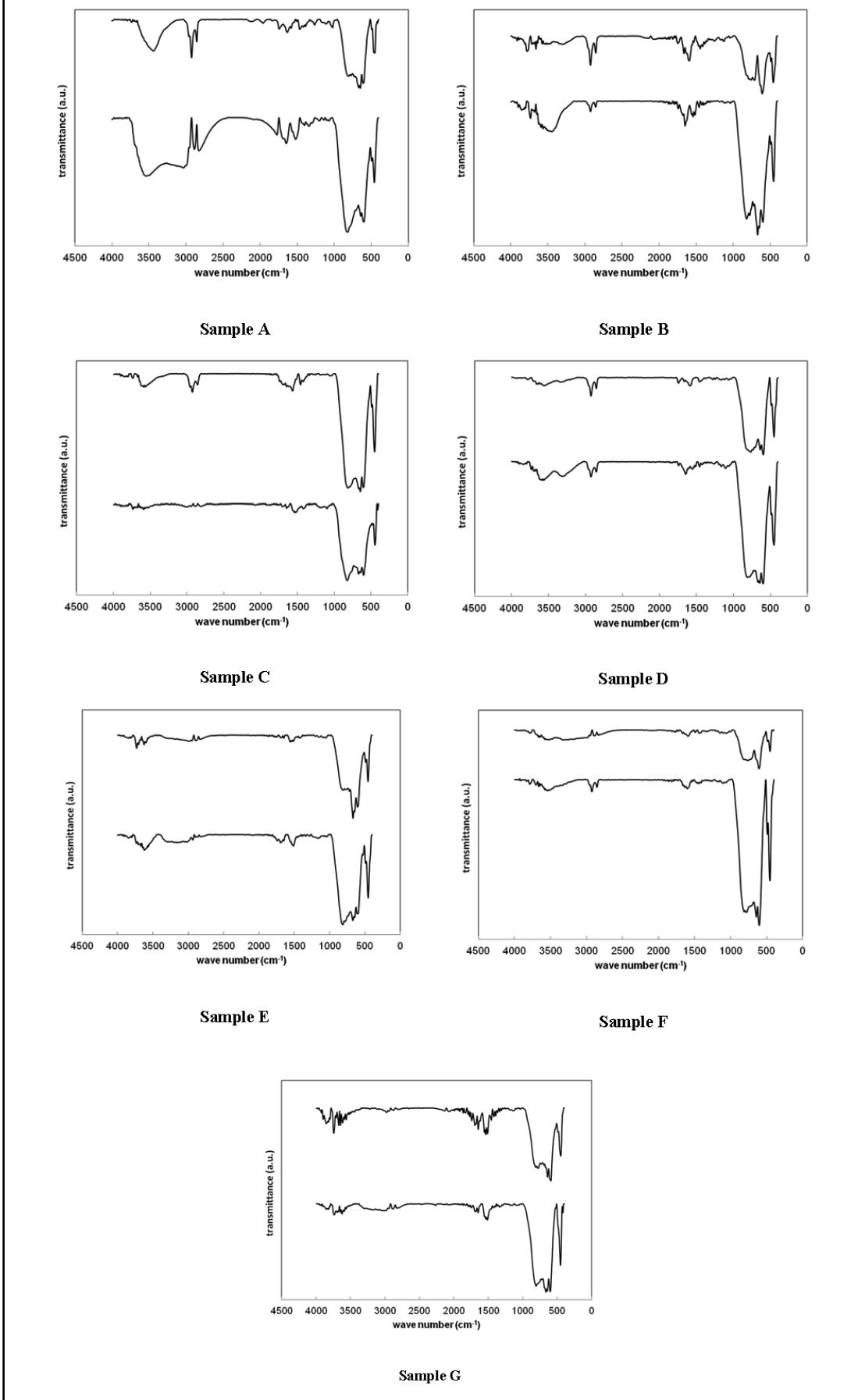


Figure 5. FT-IR graph of fresh (lower chart) and spent (upper chart) samples

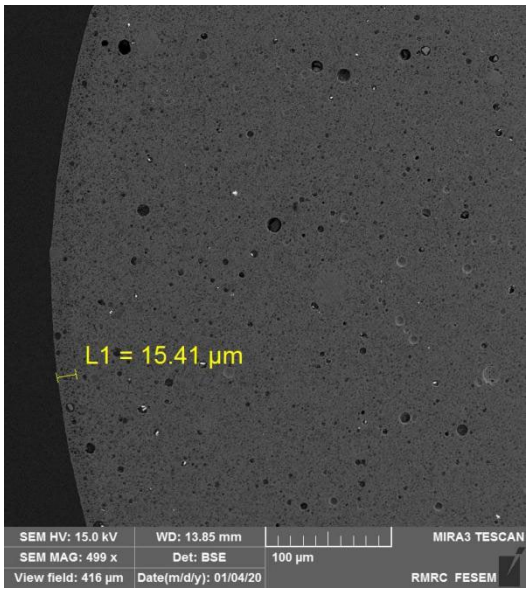
4. Conclusions

The colloidal reduction-deposition-based Pd nanoparticles stabilized by HHDMA on alumina support is a promising noble catalyst for chemoselective hydrogenation of alkynes to alkenes. In acetylene hydrogenation to ethylene, the incorporation of ligand increases the ethylene selectivity and reduces green oil (oligomeric by-products being coke precursor) at the expense of some activity loss. In addition to modification of Pd by geometric and electronic effect, the catalyst shows egg-shell distribution which is the desirable active metal distribution for selective semi-hydrogenation of acetylene. Due to low temperature of HHDMA dissociation, the regeneration procedure of these catalysts needs further research.

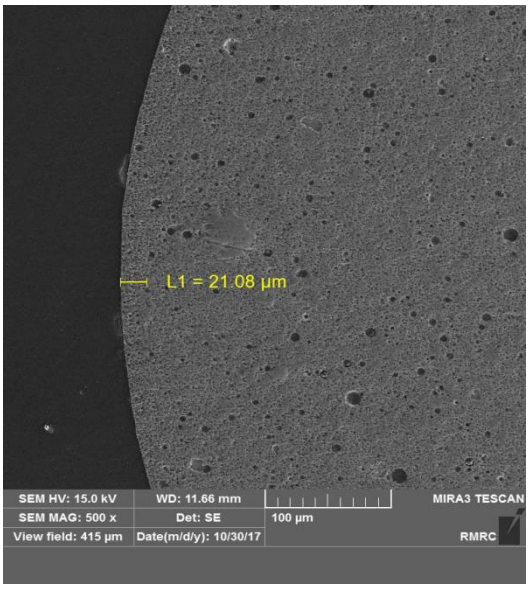
Conflict of interest

There is no conflict of interest for this study.

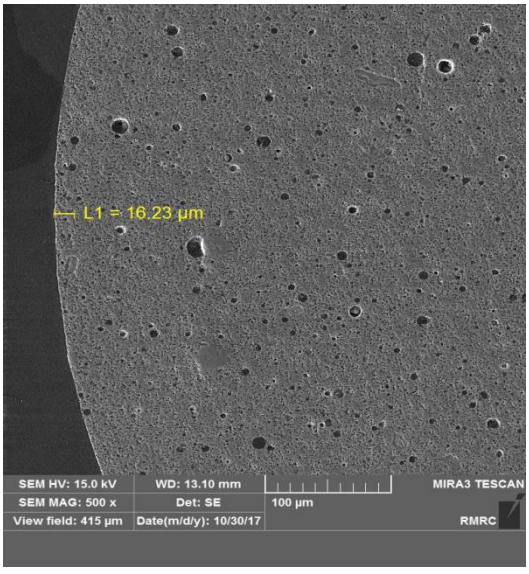
Appendix



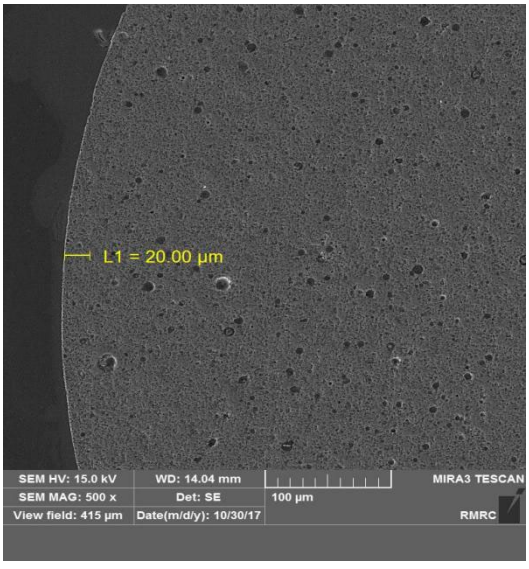
Sample A



Sample B



Sample C



Sample D

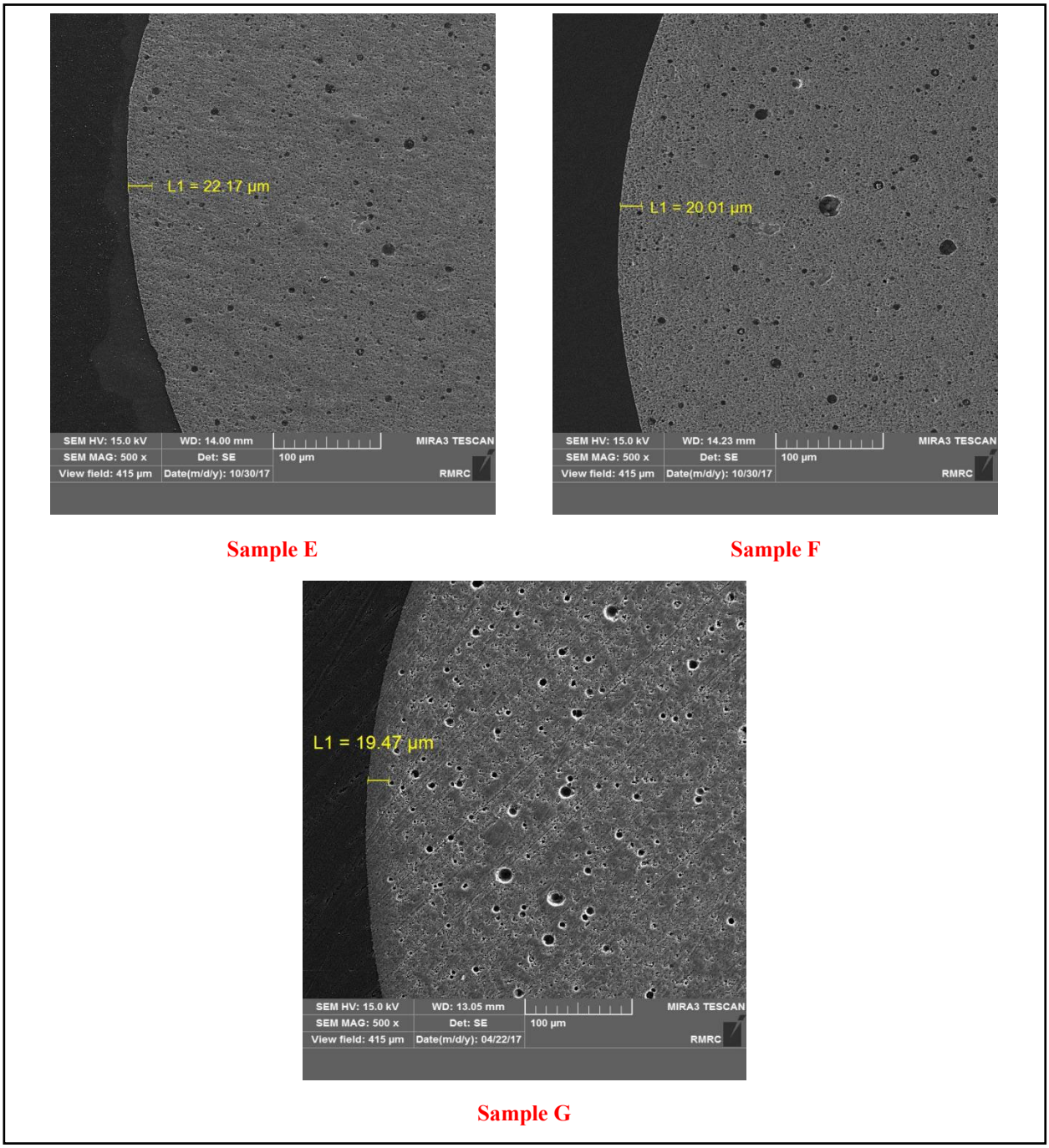


Figure A1. Pd penetration depth for the synthesized samples determined by FESEM analysis

References

[1] Delgado JA, Benkirane O, Claver C, Curulla-Ferré D, Godard C. Advances in the preparation of highly selective nanocatalysts for the semi-hydrogenation of alkynes using colloidal approaches. *Dalton Transactions*. 2017; 46: 12381-12403. https://doi.org/10.1039/C7DT01607G.

[2] Vilé G, Albani D, Almora-Barrios N, López N, Pérez-Ramírez J. Advances in the design of nanostructured catalysts for selective hydrogenation. *ChemCatChem*. 2016; 8(1): 21-33. https://doi.org/10.1002/cctc.201501269

[3] Borodzinski A, Bond GC. Selective hydrogenation of ethyne in ethene-rich streams on palladium catalysts. Part 1. Effect of changes to the catalyst during reaction. *Catalysis Reviews Science and Engineering*. 2006; 48(2): 91-144. https://doi.org/10.1080/01614940500364909

[4] Segura Y, Lûpez N, Perez-Ramirez J. Origin of the superior hydrogenation selectivity of gold nanoparticles in alkyne + alkene mixtures: Triple- versus double-bond activation. *Journal of Catalysis*. 2007; 247(2): 383-386. https://doi.org/10.1016/j.jcat.2007.02.019

[5] Ballesteros-Soberanas J, Carrasco JA, Leyva-Perez A. Parts-per-millions of soluble Pd^0 catalyze the semi-hydrogenation reaction of alkynes to alkenes. *Journal of Organic Chemistry.* 2023; 88(1): 18-26. https://doi.org/10.1021/acs.joc.2c00616

[6] Ballesteros-Soberanas J, Hernandez-Garrido JC, Ceron-Carrasco JP, Leyva-Perez A. Selective semi-hydrogenation of internal alkynes catalyzed by Pd-$CaCO_3$ clusters. Journal of Catalysis. 2022; 408: 43-55. https://doi.org/10.1016/j.jcat.2022.02.020

[7] Bridier B, Lûpez N, Perez-Ramirez J. Molecular understanding of alkyne hydrogenation for the design of selective catalysts. *Dalton Transactions*. 2010; 39: 8412-8419. https://doi.org/10.1039/C0DT00010H

[8] Garcia-Mota M, Bridier B, Prez-Ramirez J, Lûpez N. Interplay between carbon monoxide, hydrides, and carbides in selective alkyne hydrogenation on palladium. *Journal of Catalysis*. 2010; 273(2): 92-102. https://doi.org/10.1016/j.jcat.2010.04.018

[9] Albani D, Shahrokhi M, Chen Z, Mitchell S, Hauert R, López N, Pérez-Ramírez J. Selective ensembles in supported palladium sulfide nanoparticles for alkyne semi-hydrogenation. *Nature Communication*. 2018; 9: 2634. https://doi.org/10.1038/s41467-018-05052-4

[10] Teschner D, Borsodi J, Wootsch A, R¦vay Z, Hvecker M, Knop-Gericke A, Jackson SD, Schlçgl R. The roles of subsurface carbon and hydrogen in palladium-catalyzed alkyne hydrogenation. *Science*. 2008; 320(5872): 86-89. https://doi.org/10.1126/science.1155200

[11] Garcia-Mota M, Gûmez-Diaz J, Novell-Leruth G, Vargas-Fuentes C, Bellarosa L, Bridier B, Perez-Ramirez J, Lûpez N. A density functional theory study of the 'mythic' Lindlar hydrogenation catalyst. *Theoretical Chemistry Accounts.* 2011; 128: 663-673. https://doi.org/10.1007/s00214-010-0800-0

[12] Witte PT, Berben PH, Boland S, Boymans EH, Vogt D, Geus JW, Donkervoort JG. BASF nanoSelect™ technology: Innovative supported Pd- and Pt-based catalysts for selective hydrogenation reactions. *Topics in Catalysis*. 2012; 55(7-10): 505-511. https://doi.org/10.1007/s11244-012-9818-y

[13] Witte PT, de Groen M, de Rooij RM, Bakermans P, Donkervoort HG, Berben PH, Geus JW. Highly active and selective precious metal catalysts by use of the reduction-deposition method. *Studies in Surface Science and Catalysis*. 2010; 175: 135-143. https://doi.org/10.1016/S0167-2991(10)75017-5

[14] Albani D, Vilé G, Mitchell S, Witte PT, Barrios NA, Verel R, López N, Ramírez J P. Ligand ordering determines the catalytic response of hybrid palladium nanoparticles in hydrogenation. *Catalysis Science and Technology*. 2016; 6: 1621-1631. https://doi.org/10.1039/C5CY01921D

[15] Witte PT, Boland S, Kirby F, van Maanen R, Bleeker BF, de Winter DAM, Post JA, Geus JW, Berben PH. NanoSelect Pd catalysts: What causes the high selectivity of these supported colloidal catalysts in alkyne semi-hydrogenation? *ChemCatChem*. 2013; 5(2): 582-587. https://doi.org/10.1002/cctc.201200460

[16] Takht Ravanchi M, Sahebdelfar S, Rahimi Fard M, Fadaeerayeni S, Bigdeli P. Pd-Ag/α-Al_2O_3 catalyst deactivation in acetylene selective hydrogenation process. *Chemical Engineering and Technology*. 2016a; 39(2): 301-310. https://doi.org/10.1002/ceat.201400526

[17] Takht Ravanchi M, Fadaeerayeni S, Rahimi Fard M. The effect of calcination temperature on physicochemical properties of alumina as a support for acetylene selective hydrogenation catalyst. *Research on Chemical Intermediates*. 2016b; 42: 4797-4811. https://doi.org/10.1007/s11164-015-2320-y

[18] Zhu Q, Gao J, Chen J, Wen L. Selective hydrogenation of acetylene over egg-shell palladium nano-catalyst. *Journal of Nanoscience and Nanotechnology*. 2010; 10(9): 5641-5647. https://doi.org/10.1166/jnn.2010.2472

[19] Khan NA, Uhl A, Shaikhutdinov S, Freund HJ. Alumina supported model Pd-Ag catalysts: A combined STM, XPS, TPD and IRAS study. *Surface Science*. 2006; 600(9): 1849-1853. https://doi.org/10.1016/j.susc.2006.02.016

[20] Kim SK, Kim C, Lee JH, Kim J, Lee H, Moon SH. Performance of shape-controlled Pd nanoparticles in the selective hydrogenation of acetylene. *Journal of Catalysis*. 2013; 306: 146-154. https://doi.org/10.1016/j.jcat.2013.06.018

[21] da Silva FP, Luiz Fiorio J, Rossi LM. Tuning the catalytic activity and selectivity of Pd nanoparticles using ligand-modified supports and surfaces. *ACS Omega*. 2017; 2(9): 6014-6022. https://doi.org/10.1021/acsomega.7b00836

[22] Sangkham T, Mekasuwandumrong O, Praserthdam P, Panpranot J. Effect of Fe-modified α-Al_2O_3 on the properties of Pd/α-Al_2O_3 catalysts in selective acetylene hydrogenation. *Reaction Kinetics and Catalysis Letters.* 2009; 97: 115-123. https://doi.org/10.1007/s11144-009-0010-8

[23] Takht Ravanchi M, Sahebdelfar S. Pd-Ag/Al_2O_3 catalyst: Stages of deactivation in tail-end acetylene selective hydrogenation. *Applied Catalysis A General.* 2016c; 525: 197-203. https://doi.org/10.1016/j.apcata.2016.07.014
[24] Woo KJ, Sang MH. Modified Pd catalysts for the selective hydrogenation of acetylene. *Catalysis Today*. 2012; 185(1): 2-16. https://doi.org/10.1016/j.cattod.2011.09.037
[25] Li DY, Lin YS, Li YC, Shieh DL, Lin JL. Synthesis of mesoporous pseudoboehmite and alumina templated with 1-hexadecyl-2,3-dimethyl-imidazolium chloride. *Microporous and Mesoporous Materials*. 2008; 108(1-3): 276-282. https://doi.org/10.1016/j.micromeso.2007.04.009
[26] Liu C, Shih K, Gao Y, Li F, Wei L. Dechlorinating transformation of propachlor through nucleophilic substitution by dithionite on the surface of alumina. *Journal of Soils Sediments*. 2012; 12: 724-733. https://doi.org/10.1007/s11368-012-0506-0
[27] Zu G, Shen J, Wei X, Ni X, Zhang Z, Wang J, Liu G. Preparation and characterization of monolithic alumina aerogels. *Journal of Non-Crystalline Solids*. 2011; 357(15): 2903-2906. https://doi.org/10.1016/j.jnoncrysol.2011.03.031
[28] Kozhevnikov IV, Holmes S, Siddiqui MRH. Coking and regeneration of $H_3PW_{12}O_{40}/SiO_2$ catalysts. *Applied Catalysis A General*. 2001; 214(1): 47-58. https://doi.org/10.1016/S0926-860X(01)00469-0